Research Article **Open Access**

Ann Britt Petermann*, Bernhard Roth, Uwe Morgner, and Merve Meinhardt-Wollweber

All-polymer whispering gallery mode sensor for application in optofluidics

DOI 10.1515/odps-2017-0002
Received December 16, 2016; revised April 10, 2017; accepted April 22, 2017

Abstract: Microcavities such as spheres or rings are resonant optical sensors which support whispering gallery modes (WGMs). In recent years WGM based sensors have been continuously improved with respect to sensitivity and detection limit. The conventional method to measure physical as well as biological quantities using WGMs is to record the resonance shift of a single resonator. To ensure high sensitivity, resonators with high quality factors, expensive ultranarrow-linewidth tunable laser systems, and piezoelectric positioning are necessary. All these requirements hamper operation beyond the laboratory environment. To overcome these limitations in previous work we presented a small and completely polymer based measurement system. We use an array of microspheres with slightly different diameters, taking advantage of the fact that every single microsphere has a different resonance behaviour. Using many spheres instead of a single one relieves the high demands on resonator quality and allows using inexpensive polymer spheres instead of high quality resonators. Here we show, that a fixation of the spheres makes the device more robust with the result that the sensor is well suited for the determination of an unknown wavelength under different environmental conditions, for example in aqueous environment. This offers the possibility to use the sensor in microfluidics in the future.

Keywords: Polymers, Spectrometers and spectroscopic instrumentation, Integrated optics devices

***Corresponding Author: Ann Britt Petermann:** Hannover Centre for Optical Technologies (HOT), Leibniz University Hannover, Nienburger Strasse 17, 30167 Hannover, Germany, E-mail: ann-britt.petermann@hot.uni-hannover.de
Bernhard Roth: Hannover Centre for Optical Technologies (HOT), Leibniz University Hannover, Nienburger Strasse 17, 30167 Hannover, Germany, E-mail: bernhard.roth@hot.uni-hannover.de
Uwe Morgner: Institute of Quantum Optics, Leibniz University Hannover, Welfengarten 1, 30167 Hannover, Germany, E-mail: morgner@iqo.uni-hannover.de
Merve Meinhardt-Wollweber: Hannover Centre for Optical Technologies (HOT), Leibniz University Hannover, Nienburger Strasse 17, 30167 Hannover, Germany, E-mail: merve.wollweber@hot.uni-hannover.de.edu

1 Introduction

In the 19th century Lord Rayleigh described the phenomenon of whispering gallery-modes in the St. Paul's Cathedral in London [1]. Visitors can talk to each other in a whisper along the whole gallery of the dome with a diameter of 32 meter. The sound is an acoustic wave, which is guided close to the surface due to continuous reflection. A comparable effect occurs for light waves. In optical resonators, that have a closed concave structure, such as rings, spheres or toroids, light waves can interfere constructively with themselves after one round trip. The corresponding wavelengths are resonance wavelengths and they are called whispering gallery modes too, similar to the sound waves in St Paul's Cathedral [2]. Neglecting losses such as scattering or absorption, the light would circulate in the resonator forever. If losses are present, the real lifetime is described by the quality factor (or Q-factor) of the resonator [3]. The Q-factor is proportional to the relationship between the energy stored in the resonator and the dissipation. Alternatively the Q-factor can qualified by the ratio between resonance wavelength and the width of the resonance [2]. In recent years WGM based resonators are increasingly used as sensors, because changing the environment of the resonator, be it by adsorption of molecules [4] or variation in the temperature [5], causes a resonance wavelength shift. The detection limit increases, if the detectable resonance shift becomes smaller. The larger the free spectral range (distance between neighbouring modes) and the narrower the full-width-at-half-maximum (FWHM), the easier a resonance shift can be detected.
In the last few years WGM based sensors are continuously enhanced with respect to detection limit and sensitivity [6, 7]. Nevertheless the realised sensors are often large in size and complex for real world applications [8]. With the goal to realize a robust and easy to fabricate sensor, a completely polymer based sensor was developed [9], based on a concept, first presented by Schweiger et al. [10–13]. The

underlying principle is the following: An array of polymer micro-spheres is placed on a microscope slide or a prism. The microscope slide or the prism acts as a waveguide, when a laser is coupled to it. At the surface an evanescent field is generated and the micro-spheres are placed in close proximity to this field. Images of the array are taken at each wavelength step, when the laser is scanned. Only some spheres are in resonance at a given wavelength, because the spheres vary in size, see figure 1.

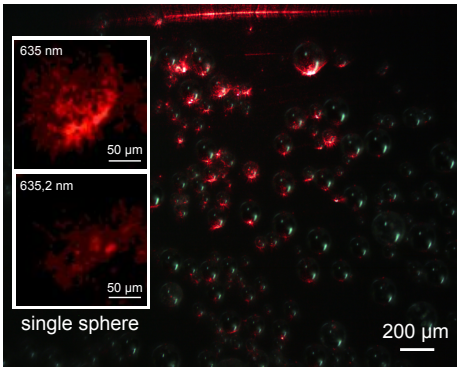

Figure 1: The spheres placed in the evanescent field generated by a red laser (635 nm) are excited. Additionally the array is illuminated from above for better visibility. The inset shows a magnification of a single sphere for two different wavelengths.

The obtained values are used as a reference. To determine an unknown wavelength the intensity distribution of the array at the unknown wavelength is compared to the reference data. So the fundamental idea is to apply many resonators instead of just one and to take advantage of this multiplexing approach to minimize sensitivity losses compared to established systems. In this work, we demonstrate that the sensor approach can be used for wavelength detection in different environments, i.e. gases or liquids.

2 Experimental Setup

Figure 2 shows a sketch of the realized sensor system. A tunable laser (TLB-6700, Newport Spectra-Physics GmbH, Darmstadt, Germany) is collimated and coupled under 45° to a PMMA substrate (with dimensions 50 mm × 50 mm × 2 mm). The light is guided in the substrate due to total internal reflection. At the spots where the beam is reflected an evanescent field is present. In this portion of the field commercially available PMMA spheres (Bangs Laboratories, Indiana, USA) are placed with a random distribution and position. If necessary the spheres can be fixed to the substrate [14]. The intensity distribution of the spheres is captured with a CMOS camera.

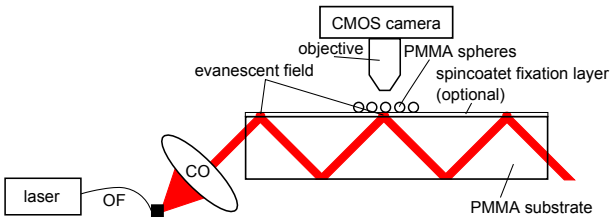

Figure 2: Sketch of the experimental setup: A tunable laser is coupled under 45° in a PMMA substrate (OF: optical fiber, CO: collimation optic). The light is guided due to total internal reflection. The spheres are placed in the evanescent field present at the surface. The light distribution is captured by a CMOS camera equipped with a microscope objective. If required the spheres can be fixed to the substrate with a spin-coated adhesive layer.

The mean sphere diameter is 165 µm (diameters between 150 µm-180 µm). Since the sphere diameter vary only some spheres are in resonance when the laser wavelength is scanned to excite them. Therefore an individual spatial intensity sphere profile belongs to each wavelength. Furthermore a suitable fixation of the spheres on the substrate and a fluidic cell were developed, to allow operation in a tubulent or windy environment. For the fixation a UV curable resin (OG675, John P. Kummer GmbH, Augsburg, Germany) was used. It was spin-coated (12 000 rpm for 4 min) on the substrate and subsequently the spheres were pressed in the layer and the resin was cured for 10 min at 365 nm with an intensity of 4 µW [14].

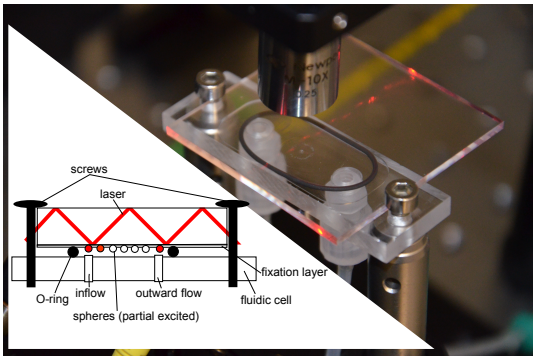

Figure 3: Fluidic cell (left: schematic, right: photograph): The spheres are fixed to the substrate. The substrate is placed on top of the fluidic cell so that the spheres are in the channel. The fluidic cell has two ports (inward and outward flow). The sealing was ensured by an O-ring and the substrate is fixed to the cell via two screws.

To ensure, that the light is still guided in the substrate by total internal reflection, the refractive index has to be smaller than the one of the PMMA spheres and the substrate. This requirement is fulfilled, because the spin coated layer has a refractive index of 1.488 at a wavelength of 639 nm. The fluidic cell has two ports, one inward and one outward flow (see figure 3). The PMMA substrate with fixed spheres is inverted and placed over the fluidic cell channel in such a way, that the spheres are in the channel. The sealing was ensured by an O-ring.

3 Calibration

Before the sensor can be used to measure an unknown wavelength for example, it needs to be calibrated once.

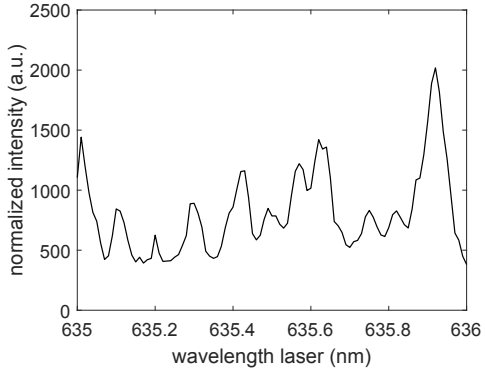

(a) Resonance spectrum

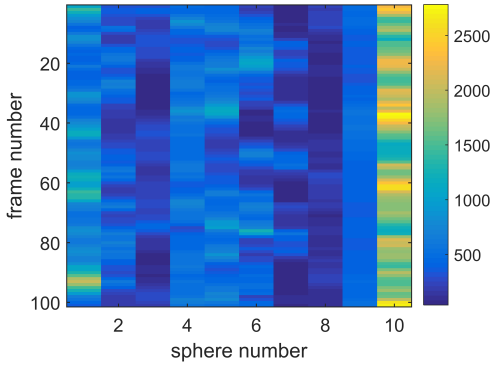

(b) Modemap

Figure 4: (a) Spectrum for one exemplary sphere. (b) Modemap: Intensities of all spheres (here ten spheres). Frame number correlates to wavelength.

Therefore the laser is tuned from 635 nm to 636 nm in steps of 0.01 nm. The intensity profile formed by the spheres is captured with the CMOS camera at each wavelength. Figure 4(a) shows the resonance spectrum of one exemplary sphere. The intensity profiles at all wavelengths are compiled to a modemap, shown in figure 4(b).
An unknown wavelength can be determined by measuring the intensity profile of the spheres at the unknown wavelength. Then this profile is compared to the modemap via the correlation function $r(\lambda)$ [9, 12]:

$$r(\lambda) = \sum_{j=1}^{N} |I_j^{DB}(\lambda) - I_j|. \tag{1}$$

Here, I_j^{DB} is the intensity of the j-th sphere in the modemap, I_j the intensity of this sphere at the unknown wavelength and N the sphere number. The correlation function has a minimum at the unknown wavelength (see figure 5).

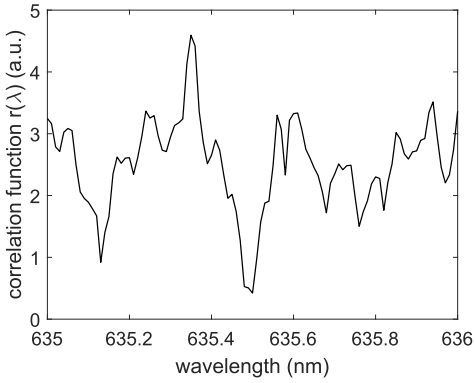

Figure 5: At the real wavelength of 635.5 nm the correlation function $r(\lambda)$ has a minimum (in this case $N = 10$).

4 Measurement

To demonstrate, that the sensor system can be used to determine an unknown wavelength in diverse surroundings, it was tested in air with and without a fixation of the spheres and also in the fluidic cell with and without water. For each configuration the laser was scanned twice. With the first scan the modemap was build. Afterwards the correlation function was calculated for each wavelength of the second scan and the modemap. The resultant wavelengths are compared to the true wavelength values.

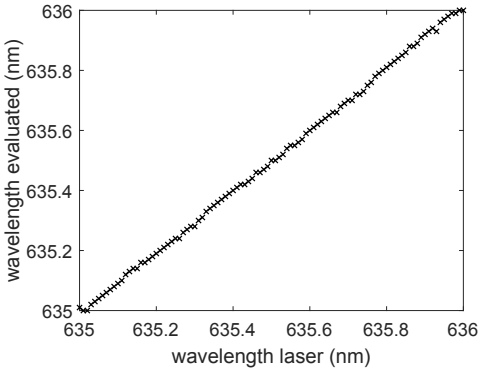

(a) without fixation in air

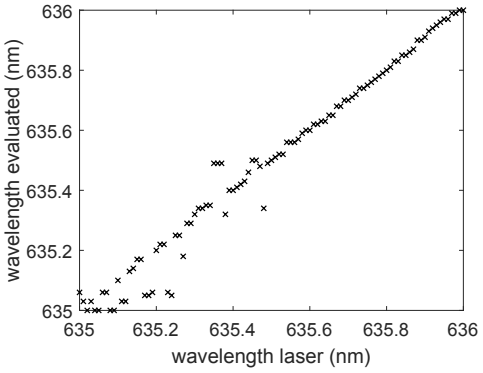

(b) with fixation in air

Figure 6: Determination of unknown wavelength for different sensor configurations. Each sensor contains a different number of spheres: (a) $N = 10$ and (b) $N = 12$.

Figure 6 shows the result for a sensor without fixed spheres (a) and with fixed spheres (b) and figure 7 in the fluidic cell without water (a) and with water (b), respectively. Obviously the accuracy of the wavelength determination differs between the different configurations. To measure the accuracy A we use the following equation:

$$A = \sqrt{\frac{1}{M}\sum_{i=1}^{M}(\lambda_i - \lambda_r)^2}. \qquad (2)$$

Here, λ_i is the evaluated wavelength, λ_r is the real wavelength and M the number of scanning steps.

Table 1 shows the accuracy for the different sensor configurations. The best results can be achieved in air without a fixation, because in this case no disturbing fixation layer is present. The adjustment of the fixation layer thickness is a delicate issue [14, 15]. There is an optimal gap size between resonator and excitation source depending on sphere size, type of excitation source as well as refractive indices of resonator and gap medium [15, 16]. In case of an optimal gap the coupling between resonator and excitation source becomes maximal (called critical coupling) and the quality factor achieves its highest possible value [17]. The fixation layer used in this work does not allowed a precise adjustment between resonator and source. Nevertheless we showed in [14], that these disadvantages can partly be compensated by adding additional spheres. This fact can also be observed in figure 6.

Table 1: Accuracy of the wavelength determination (nm).

sensor configuration	accuracy A
without fixation in air	0.010
with fixation in air	0.049
without water in the fluidic cell	0.043
with water in the fluidic cell	0.197

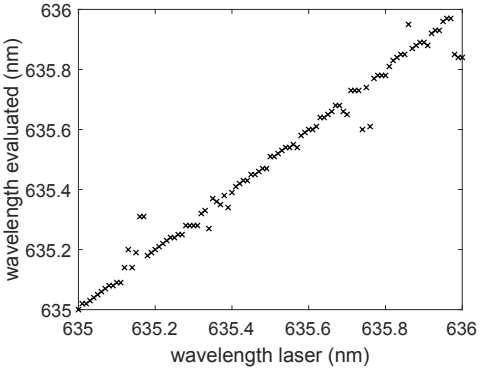

(a) without water in the fluidic cell/fixed spheres

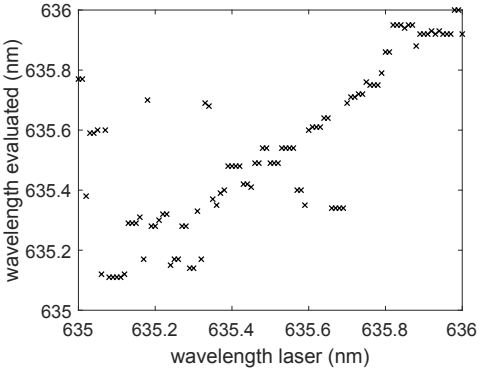

(b) with water in the fluidic cell/fixed spheres

Figure 7: Determination of unknown wavelength for different sensor configurations. Each sensor contains a different number of spheres: (a) $N = 20$ and (b) $N = 8$.

For the calculation of figure 6(b) as well as for figure 7(a) a sensor with fixation layer was used. However the sensors differ in sphere number (figure 6(b) $N = 12$ and figure 7(a) $N = 20$). Although the sensor in figure 7(a) was further adapted to a fluidic cell the determination of unknown wavelength was more precise simply by applying more spheres. The precision of the wavelength determination in water is somewhat lower. Nevertheless as figure 7(b) shows, the trend is correct. So as mentioned above, it should be possible to improve the sensor sensitivity in fluidic environments by adding more spheres or changing the sphere radius. Unfortunately the fluidic cell used was too small to test this. The next version of our fluidic cell will enable such tests in future.

The sensor array can also be used for temperature measurements. The calibration process is similar to the one explained above. The temperature is scanned in defined steps. A picture of the array is taken at each step and the intensity changes of all spheres are stored together in a modemap. To measure an unknown temperature the intensity profile at this temperature is compared with the modemap by a correlation function:

$$r(T) = \sum_{j=1}^{N} |I_j^{DB}(T) - I_j|. \tag{3}$$

Here, I_j^{DB} is the intensity of the j-th sphere in the modemap, I_j the intensity of this sphere at the unknown temperature and N the sphere number. The correlation function has a minimum at the unknown temperature. We can reach a temperature sensitivity of $0.001\,\mathrm{nm\,K^{-1}}$ with our sensor [9]. Moreover the temperature scan in the calibration process can be replaced by a wavelength scan [11].

5 Conclusion

We present a small-volume and completely polymer based measurement device for the determination of an unknown wavelength on the basis of the evaluation of optical resonances in polymer micro-spheres. We demonstrate that the device can be extended by a fixation layer making the determination of an unknown wavelength in a wide range of environments feasible. For example the sensor can be adapted to a fluidic cell to enable measurements in aqueous solutions. Moreover the sensor is inexpensive and easy to manufacture. The accuracy depends on several factors: the dependence on the number and mean size of the spheres in the presence or absence of a fixation layer is discussed here and related to this the achievable Q-factor or coupling efficiency. Using many spheres lowers the demands on a precise adjustment of the fixation layer thickness and the resonator quality. Currently the scanning step used for building the modemap limits the accuracy for the determination of an unknown wavelength and the scanning range restricts the possible wavelength region of the unknown source to be measured. The next steps are to build an advanced fluidic cell, validate the sensor for measurement of other physical quantities, and develop a suitable functionalization for biosensing applications. Moreover it might be necessary to change the fixation layer material for measurements in aqueous environments, because the quality factor of the spheres is higher the better the refractive index of the layer is matched to the refractive index of water [18].

Acknowledgement: The authors gratefully acknowledge the financial support by Deutsche Forschungsgesellschaft (DFG) within the Collaborative Research Center "Transregio 123 - Planar Optronic Systems."

References

[1] J.W.S. Rayleigh, Philosophical Magazine 20, 1001—1004 (1910)
[2] M.R. Foreman, J.D. Swaim, F. Vollmer, Advances in Optics and Photonics 7, 267–291 (2015)
[3] F. Vollmer, L. Yang, Nanophotonics 1, 267–291 (2012)
[4] S. Arnold, M. Khoshsima, I. Teraoka, S. Holler, F. Vollmer, Optics Letters 28, 272–274 (2003)
[5] D.V. Strekalov, R.J. Thompson, L.M. Baumgartel, I.S. Grudinin, N. Yu, Optics Express 19, 14495–14501 (2011)
[6] B.Q. Shen, X.C. Yu, Y. Zhi, L. Wang, D. Kim, Q. Gong, Y.F. Xiao, Phys. Rev. Applied 5, 024011 (2016)
[7] F. Vollmer, S. Arnold, Nature methods 5, 591–596 (2008)
[8] H. Ghali, H. Chibli, J.L. Nadeau, P. Bianucci, Y.A. Peter Biosensors 6, 20 (2016)
[9] A.B. Petermann, A. Varkentin, B. Roth, U. Morgner, M. Meinhardt-Wollweber, Optics Express 24, 6052–6062 (2016)
[10] T. Weigel, R. Nett, G. Schweiger, SPIE proceeding 73660, 73660H (2009)
[11] T. Weigel, H. Dobbelstein, C. Esen, G. Schweiger, A. Ostendorf, SPIE Proceeding 89600, 89600H (2014)
[12] T. Weigel, R. Nett, G. Schweiger, A. Ostendorf, SPIE Proceeding 77260, 77260C (2010)
[13] G. Schweiger, R. Nett, T. Weigel, Optics Letters 32, 2644–2646 (2007)
[14] A.B. Petermann, M. Rezem, B. Roth, U. Morgner, M. Meinhardt-Wollweber, Sensors and Actuators A: Physical, (2016)
[15] L.M. Gorodetsky, V.S. Ilchenko, J. Opt. Soc. Am. B 16, 147–154 (1999)
[16] D.V. Tishinin, P.D. Dapkus, A.E. Bond, I. Kim, C.K. Lin, J. O'brien, IEEE Photon. Technol. Lett. 11, 1003–1005 (1999)
[17] M. Cai, O. Painter, K.J. Vahala, Phys. Rev. Lett. 85, 74 (2000)
[18] J. Lutti, L. Langbein, P. Borri, Physics Letters 93, 151103 (2008)